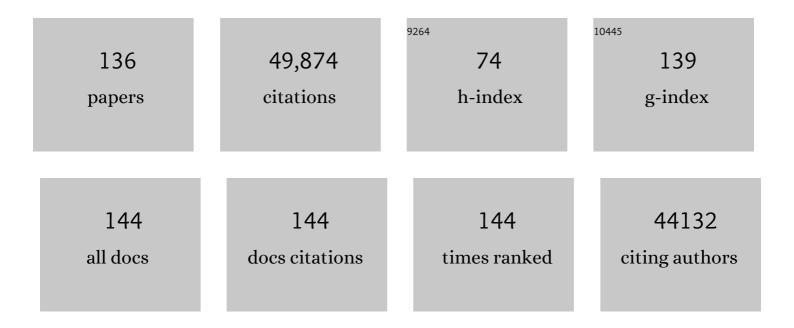
## Yongye Liang

List of Publications by Year in descending order

Source: https://exaly.com/author-pdf/5944825/publications.pdf Version: 2024-02-01



#	Article	IF	CITATIONS
1	Co3O4 nanocrystals on graphene as a synergistic catalyst for oxygen reduction reaction. Nature Materials, 2011, 10, 780-786.	27.5	5,120
2	MoS <sub>2</sub> Nanoparticles Grown on Graphene: An Advanced Catalyst for the Hydrogen Evolution Reaction. Journal of the American Chemical Society, 2011, 133, 7296-7299.	13.7	4,572
3	For the Bright Future—Bulk Heterojunction Polymer Solar Cells with Power Conversion Efficiency of 7.4%. Advanced Materials, 2010, 22, E135-8.	21.0	3,509
4	Polymer solar cells with enhanced open-circuit voltage and efficiency. Nature Photonics, 2009, 3, 649-653.	31.4	3,015
5	An Advanced Ni–Fe Layered Double Hydroxide Electrocatalyst for Water Oxidation. Journal of the American Chemical Society, 2013, 135, 8452-8455.	13.7	2,498
6	Graphene-Wrapped Sulfur Particles as a Rechargeable Lithium–Sulfur Battery Cathode Material with High Capacity and Cycling Stability. Nano Letters, 2011, 11, 2644-2647.	9.1	1,973
7	Ultrasmall Reduced Graphene Oxide with High Near-Infrared Absorbance for Photothermal Therapy. Journal of the American Chemical Society, 2011, 133, 6825-6831.	13.7	1,897
8	Ni(OH) <sub>2</sub> Nanoplates Grown on Graphene as Advanced Electrochemical Pseudocapacitor Materials. Journal of the American Chemical Society, 2010, 132, 7472-7477.	13.7	1,865
9	Mn <sub>3</sub> O <sub>4</sub> â^`Graphene Hybrid as a High-Capacity Anode Material for Lithium Ion Batteries. Journal of the American Chemical Society, 2010, 132, 13978-13980.	13.7	1,849
10	An oxygen reduction electrocatalyst based on carbon nanotube–graphene complexes. Nature Nanotechnology, 2012, 7, 394-400.	31.5	1,533
11	Highly Efficient Solar Cell Polymers Developed via Fine-Tuning of Structural and Electronic Properties. Journal of the American Chemical Society, 2009, 131, 7792-7799.	13.7	1,339
12	Covalent Hybrid of Spinel Manganese–Cobalt Oxide and Graphene as Advanced Oxygen Reduction Electrocatalysts. Journal of the American Chemical Society, 2012, 134, 3517-3523.	13.7	1,266
13	Advanced zinc-air batteries based on high-performance hybrid electrocatalysts. Nature Communications, 2013, 4, 1805.	12.8	976
14	Development of New Semiconducting Polymers for High Performance Solar Cells. Journal of the American Chemical Society, 2009, 131, 56-57.	13.7	904
15	Strongly Coupled Inorganic/Nanocarbon Hybrid Materials for Advanced Electrocatalysis. Journal of the American Chemical Society, 2013, 135, 2013-2036.	13.7	856
16	Oxygen Reduction Electrocatalyst Based on Strongly Coupled Cobalt Oxide Nanocrystals and Carbon Nanotubes. Journal of the American Chemical Society, 2012, 134, 15849-15857.	13.7	747
17	TiO2 nanocrystals grown on graphene as advanced photocatalytic hybrid materials. Nano Research, 2010, 3, 701-705.	10.4	693
18	A New Class of Semiconducting Polymers for Bulk Heterojunction Solar Cells with Exceptionally High Performance. Accounts of Chemical Research, 2010, 43, 1227-1236.	15.6	674

#	Article	IF	CITATIONS
19	Domino electroreduction of CO2 to methanol on a molecular catalyst. Nature, 2019, 575, 639-642.	27.8	658
20	Highly selective and active CO2 reduction electrocatalysts based on cobalt phthalocyanine/carbon nanotube hybrid structures. Nature Communications, 2017, 8, 14675.	12.8	618
21	Synthesis of Fluorinated Polythienothiophene- <i>co</i> -benzodithiophenes and Effect of Fluorination on the Photovoltaic Properties. Journal of the American Chemical Society, 2011, 133, 1885-1894.	13.7	548
22	Active sites of copper-complex catalytic materials for electrochemical carbon dioxide reduction. Nature Communications, 2018, 9, 415.	12.8	527
23	Co <sub>1â~`<i>x</i></sub> S–Graphene Hybrid: A Highâ€Performance Metal Chalcogenide Electrocatalyst for Oxygen Reduction. Angewandte Chemie - International Edition, 2011, 50, 10969-10972.	13.8	413
24	Rechargeable Li–O2 batteries with a covalently coupled MnCo2O4–graphene hybrid as an oxygen cathode catalyst. Energy and Environmental Science, 2012, 5, 7931.	30.8	393
25	Advanced asymmetrical supercapacitors based on graphene hybrid materials. Nano Research, 2011, 4, 729-736.	10.4	390
26	Donor Engineering for NIR-II Molecular Fluorophores with Enhanced Fluorescent Performance. Journal of the American Chemical Society, 2018, 140, 1715-1724.	13.7	379
27	In Vivo Fluorescence Imaging in the Second Near-Infrared Window with Long Circulating Carbon Nanotubes Capable of Ultrahigh Tumor Uptake. Journal of the American Chemical Society, 2012, 134, 10664-10669.	13.7	373
28	Molecular engineering of dispersed nickel phthalocyanines on carbon nanotubes for selective CO2 reduction. Nature Energy, 2020, 5, 684-692.	39.5	365
29	Rational Design of Molecular Fluorophores for Biological Imaging in the NIRâ€II Window. Advanced Materials, 2017, 29, 1605497.	21.0	356
30	Facile Synthesis of Nickel–Iron/Nanocarbon Hybrids as Advanced Electrocatalysts for Efficient Water Splitting. ACS Catalysis, 2016, 6, 580-588.	11.2	354
31	A bright organic NIR-II nanofluorophore for three-dimensional imaging into biological tissues. Nature Communications, 2018, 9, 1171.	12.8	353
32	An ultrafast nickel–iron battery from strongly coupled inorganic nanoparticle/nanocarbon hybrid materials. Nature Communications, 2012, 3, 917.	12.8	347
33	When Function Follows Form: Effects of Donor Copolymer Side Chains on Film Morphology and BHJ Solar Cell Performance. Advanced Materials, 2010, 22, 5468-5472.	21.0	315
34	Traumatic Brain Injury Imaging in the Second Nearâ€Infrared Window with a Molecular Fluorophore. Advanced Materials, 2016, 28, 6872-6879.	21.0	311
35	Plastic Nearâ€Infrared Photodetectors Utilizing Low Band Gap Polymer. Advanced Materials, 2007, 19, 3979-3983.	21.0	281
36	Ultrafast high-capacity NiZn battery with NiAlCo-layered double hydroxide. Energy and Environmental Science, 2014, 7, 2025.	30.8	265

#	Article	IF	CITATIONS
37	LiMn <sub>1â^'<i>x</i></sub> Fe <sub><i>x</i></sub> PO <sub>4</sub> Nanorods Grown on Graphene Sheets for Ultrahighâ€Rateâ€Performance Lithium Ion Batteries. Angewandte Chemie - International Edition, 2011, 50, 7364-7368.	13.8	262
38	Molecular imaging of biological systems with a clickable dye in the broad 800- to 1,700-nm near-infrared window. Proceedings of the National Academy of Sciences of the United States of America, 2017, 114, 962-967.	7.1	230
39	Design of active nickel single-atom decorated MoS2 as a pH-universal catalyst for hydrogen evolution reaction. Nano Energy, 2018, 53, 458-467.	16.0	222
40	Ironâ€Ðoped Cobalt Monophosphide Nanosheet/Carbon Nanotube Hybrids as Active and Stable Electrocatalysts for Water Splitting. Advanced Functional Materials, 2017, 27, 1606635.	14.9	206
41	Facile Synthesis of Hollow Nickel Submicrometer Spheres. Advanced Materials, 2003, 15, 1832-1835.	21.0	198
42	Molybdenum Phosphide/Carbon Nanotube Hybrids as pHâ€Universal Electrocatalysts for Hydrogen Evolution Reaction. Advanced Functional Materials, 2018, 28, 1706523.	14.9	185
43	Ultrafast Intramolecular Exciton Splitting Dynamics in Isolated Low-Band-Gap Polymers and Their Implications in Photovoltaic Materials Design. Journal of the American Chemical Society, 2012, 134, 4142-4152.	13.7	177
44	Direct electrosynthesis of methylamine from carbon dioxide and nitrate. Nature Sustainability, 2021, 4, 725-730.	23.7	176
45	Nanometer-Sized Nickel Hollow Spheres. Advanced Materials, 2005, 17, 1995-1999.	21.0	167
46	SiRNA Delivery with PEGylated Graphene Oxide Nanosheets for Combined Photothermal and Genetherapy for Pancreatic Cancer. Theranostics, 2017, 7, 1133-1148.	10.0	165
47	Multiplexed NIRâ€II Probes for Lymph Nodeâ€Invaded Cancer Detection and Imagingâ€Guided Surgery. Advanced Materials, 2020, 32, e1907365.	21.0	163
48	Light-sheet microscopy in the near-infrared II window. Nature Methods, 2019, 16, 545-552.	19.0	151
49	3D NIRâ€II Molecular Imaging Distinguishes Targeted Organs with Highâ€Performance NIRâ€II Bioconjugates. Advanced Materials, 2018, 30, e1705799.	21.0	150
50	Engineering MoS <sub>2</sub> Basal Planes for Hydrogen Evolution via Synergistic Ruthenium Doping and Nanocarbon Hybridization. Advanced Science, 2019, 6, 1900090.	11.2	148
51	Structure, Dynamics, and Power Conversion Efficiency Correlations in a New Low Bandgap Polymer: PCBM Solar Cell. Journal of Physical Chemistry B, 2010, 114, 742-748.	2.6	145
52	Toward Highly Sensitive Polymer Photodetectors by Molecular Engineering. Advanced Materials, 2015, 27, 6496-6503.	21.0	136
53	General Construction of Molybdenumâ€Based Nanowire Arrays for pHâ€Universal Hydrogen Evolution Electrocatalysis. Advanced Functional Materials, 2018, 28, 1804600.	14.9	134
54	Nanographene–Osmapentalyne Complexes as a Cathode Interlayer in Organic Solar Cells Enhance Efficiency over 18%. Advanced Materials, 2021, 33, e2101279.	21.0	129

#	Article	lF	CITATIONS
55	Accessing Organonitrogen Compounds via C–N Coupling in Electrocatalytic CO <sub>2</sub> Reduction. Journal of the American Chemical Society, 2021, 143, 19630-19642.	13.7	129
56	Selfâ€Cleaning Catalyst Electrodes for Stabilized CO <sub>2</sub> Reduction to Hydrocarbons. Angewandte Chemie - International Edition, 2017, 56, 13135-13139.	13.8	126
57	Rational design of a super-contrast NIR-II fluorophore affords high-performance NIR-II molecular imaging guided microsurgery. Chemical Science, 2019, 10, 326-332.	7.4	124
58	Molecular Cancer Imaging in the Second Nearâ€Infrared Window Using a Renalâ€Excreted NIRâ€II Fluorophoreâ€Peptide Probe. Advanced Materials, 2018, 30, e1800106.	21.0	115
59	Development of Semiconducting Polymers for Solar Energy Harvesting. Polymer Reviews, 2010, 50, 454-473.	10.9	110
60	Selective and High Current CO <sub>2</sub> Electro-Reduction to Multicarbon Products in Near-Neutral KCl Electrolytes. Journal of the American Chemical Society, 2021, 143, 3245-3255.	13.7	108
61	Shape Controllable Preparation of PbS Crystals by a Simple Aqueous Phase Route. Crystal Growth and Design, 2004, 4, 759-764.	3.0	104
62	Engineering manganese oxide/nanocarbon hybrid materials for oxygen reduction electrocatalysis. Nano Research, 2012, 5, 718-725.	10.4	104
63	Nickel Hydr(oxy)oxide Nanoparticles on Metallic MoS <sub>2</sub> Nanosheets: A Synergistic Electrocatalyst for Hydrogen Evolution Reaction. Advanced Science, 2018, 5, 1700644.	11.2	104
64	Heterogeneous Molecular Catalysts of Metal Phthalocyanines for Electrochemical CO <sub>2</sub> Reduction Reactions. Accounts of Chemical Research, 2021, 54, 3149-3159.	15.6	102
65	Materials Design via Optimized Intramolecular Noncovalent Interactions for High-Performance Organic Semiconductors. Chemistry of Materials, 2016, 28, 2449-2460.	6.7	99
66	Cobalt oxide/nanocarbon hybrid materials as alternative cathode catalyst for oxygen reduction in microbial fuel cell. International Journal of Hydrogen Energy, 2015, 40, 3868-3874.	7.1	93
67	Headâ€ŧoâ€Head Linkage Containing Bithiopheneâ€Based Polymeric Semiconductors for Highly Efficient Polymer Solar Cells. Advanced Materials, 2016, 28, 9969-9977.	21.0	93
68	Interfacial Layer Engineering for Performance Enhancement in Polymer Solar Cells. Polymers, 2015, 7, 333-372.	4.5	86
69	A theranostic agent for cancer therapy and imaging in the second near-infrared window. Nano Research, 2019, 12, 273-279.	10.4	86
70	Developing a Bright NIRâ€II Fluorophore with Fast Renal Excretion and Its Application in Molecular Imaging of Immune Checkpoint PDâ€L1. Advanced Functional Materials, 2018, 28, 1804956.	14.9	85
71	High Performance, Multiplexed Lung Cancer Biomarker Detection on a Plasmonic Gold Chip. Advanced Functional Materials, 2016, 26, 7994-8002.	14.9	84
72	Rational Design of High Brightness NIR-II Organic Dyes with S-D-A-D-S Structure. Accounts of Materials Research, 2021, 2, 170-183.	11.7	84

#	Article	IF	CITATIONS
73	Transition-Metal Doped Ceria Microspheres with Nanoporous Structures for CO Oxidation. Scientific Reports, 2016, 6, 23900.	3.3	78
74	Conjugated block copolymers and co-oligomers: from supramolecular assembly to molecular electronics. Journal of Materials Chemistry, 2007, 17, 2183.	6.7	75
75	Revealing the hidden performance of metal phthalocyanines for CO2 reduction electrocatalysis by hybridization with carbon nanotubes. Nano Research, 2019, 12, 2330-2334.	10.4	72
76	Propylenedioxy Thiophene Donor to Achieve NIR-II Molecular Fluorophores with Enhanced Brightness. Chemistry of Materials, 2020, 32, 2061-2069.	6.7	72
77	Assessing the energy offset at the electron donor/acceptor interface in organic solar cells through radiative efficiency measurements. Energy and Environmental Science, 2019, 12, 3556-3566.	30.8	69
78	Brain imaging with near-infrared fluorophores. Coordination Chemistry Reviews, 2019, 380, 550-571.	18.8	68
79	Molecular Engineering on Conjugated Side Chain for Polymer Solar Cells with Improved Efficiency and Accessibility. Chemistry of Materials, 2016, 28, 5887-5895.	6.7	65
80	Regioregular Oligomer and Polymer Containing Thieno[3,4- <i>b</i> ]thiophene Moiety for Efficient Organic Solar Cells. Macromolecules, 2009, 42, 1091-1098.	4.8	64
81	Large-scale synthesis of single-crystalline CuO nanoplatelets by a hydrothermal process. Materials Research Bulletin, 2006, 41, 697-702.	5.2	62
82	Control in Energy Levels of Conjugated Polymers for Photovoltaic Application. Journal of Physical Chemistry C, 2008, 112, 7866-7871.	3.1	62
83	High-Performance Fullerene-Free Polymer Solar Cells Featuring Efficient Photocurrent Generation from Dual Pathways and Low Nonradiative Recombination Loss. ACS Energy Letters, 2019, 4, 8-16.	17.4	62
84	Phthalocyanine Precursors To Construct Atomically Dispersed Iron Electrocatalysts. ACS Catalysis, 2019, 9, 6252-6261.	11.2	61
85	A bio-inspired O2-tolerant catalytic CO2 reduction electrode. Science Bulletin, 2019, 64, 1890-1895.	9.0	61
86	Solution phase synthesis of CuO nanorods. Materials Chemistry and Physics, 2006, 98, 519-522.	4.0	60
87	Intraâ€Molecular Donor–Acceptor Interaction Effects on Charge Dissociation, Charge Transport, and Charge Collection in Bulkâ€Heterojunction Organic Solar Cells. Advanced Energy Materials, 2011, 1, 923-929.	19.5	58
88	Highly active oxygen evolution integrated with efficient CO <sub>2</sub> to CO electroreduction. Proceedings of the National Academy of Sciences of the United States of America, 2019, 116, 23915-23922.	7.1	58
89	Organic Spherical Nucleic Acids for the Transport of a NIRâ€llâ€Emitting Dye Across the Blood–Brain Barrier. Angewandte Chemie - International Edition, 2020, 59, 9702-9710.	13.8	58
90	Graphite-Coated Magnetic Nanoparticle Microarray for Few-Cells Enrichment and Detection. ACS Nano, 2012, 6, 1094-1101.	14.6	57

#	Article	IF	CITATIONS
91	Stable cycling of mesoporous Sn4P3/SnO2@C nanosphere anode with high initial coulombic efficiency for Li-ion batteries. Energy Storage Materials, 2019, 18, 125-132.	18.0	56
92	Magnetic "Squashing―of Circulating Tumor Cells on Plasmonic Substrates for Ultrasensitive NIR Fluorescence Detection. Small Methods, 2019, 3, 1800474.	8.6	52
93	Development of a high quantum yield dye for tumour imaging. Chemical Science, 2017, 8, 6322-6326.	7.4	51
94	Spectroscopic understanding of ultra-high rate performance for LiMn0.75Fe0.25PO4 nanorods–graphene hybrid in lithium ion battery. Physical Chemistry Chemical Physics, 2012, 14, 9578.	2.8	48
95	Thieno[3,4- <i>c</i> ]pyrrole-4,6(5 <i>H</i> )-dione Polymers with Optimized Energy Level Alignments for Fused-Ring Electron Acceptor Based Polymer Solar Cells. Chemistry of Materials, 2017, 29, 5636-5645.	6.7	43
96	PbS crystals with clover-like structure: Preparation, characterization, optical properties and influencing factors. Crystal Research and Technology, 2004, 39, 200-206.	1.3	41
97	A non-fullerene small molecule processed with green solvent as an electron transporting material for high efficiency p-i-n perovskite solar cells. Organic Electronics, 2018, 52, 200-205.	2.6	40
98	Selfâ€Cleaning Catalyst Electrodes for Stabilized CO <sub>2</sub> Reduction to Hydrocarbons. Angewandte Chemie, 2017, 129, 13315-13319.	2.0	38
99	Head-to-Head Linkage Containing Dialkoxybithiophene-Based Polymeric Semiconductors for Polymer Solar Cells with Large Open-Circuit Voltages. Macromolecules, 2017, 50, 137-150.	4.8	37
100	Hollow nickel microspheres covered with oriented carbon nanotubes and its magnetic property. Carbon, 2006, 44, 211-215.	10.3	35
101	Metal Phthalocyanine-Derived Single-Atom Catalysts for Selective CO <sub>2</sub> Electroreduction under High Current Densities. ACS Applied Materials & amp; Interfaces, 2020, 12, 33795-33802.	8.0	35
102	Visible to Near-Infrared Fluorescence Enhanced Cellular Imaging on Plasmonic Gold Chips. Small, 2016, 12, 457-465.	10.0	33
103	Proteoliposome-based full-length ZnT8 self-antigen for type 1 diabetes diagnosis on a plasmonic platform. Proceedings of the National Academy of Sciences of the United States of America, 2017, 114, 10196-10201.	7.1	31
104	In Situ Tin(II) Complex Antisolvent Process Featuring Simultaneous Quasiâ€Core–Shell Structure and Heterojunction for Improving Efficiency and Stability of Lowâ€Bandgap Perovskite Solar Cells. Advanced Energy Materials, 2020, 10, 1903013.	19.5	31
105	Hierarchical Construction of Composite Hollow Structures of Co@CoO and Their Magnetic Behavior. Journal of Physical Chemistry C, 2008, 112, 9272-9277.	3.1	28
106	Recent Advances in Interface Engineering for Planar Heterojunction Perovskite Solar Cells. Molecules, 2016, 21, 837.	3.8	28
107	Electronic Processes in Conjugated Diblock Oligomers Mimicking Low Band-Gap Polymers: Experimental and Theoretical Spectral Analysis. Journal of Physical Chemistry B, 2010, 114, 14505-14513.	2.6	27
108	Structure and dynamics correlations of photoinduced charge separation in rigid conjugated linear donor–acceptor dyads towards photovoltaic applications. New Journal of Chemistry, 2009, 33, 1497.	2.8	25

#	Article	IF	CITATIONS
109	An efficient and thickness insensitive cathode interface material for high performance inverted perovskite solar cells with 17.27% efficiency. Journal of Materials Chemistry C, 2017, 5, 5949-5955.	5.5	24
110	Rational design of conjugated side chains for high-performance all-polymer solar cells. Molecular Systems Design and Engineering, 2018, 3, 103-112.	3.4	24
111	Theory-Driven Design of Electrocatalysts for the Two-Electron Oxygen Reduction Reaction Based on Dispersed Metal Phthalocyanines. CCS Chemistry, 2022, 4, 228-236.	7.8	24
112	Methyl Thioether Functionalization of a Polymeric Donor for Efficient Solar Cells Processed from Non-Halogenated Solvents. Chemistry of Materials, 2019, 31, 3025-3033.	6.7	23
113	High brightness NIR-II nanofluorophores based on fused-ring acceptor molecules. Nano Research, 2020, 13, 2570-2575.	10.4	23
114	Fabrication and characterization of hollow cuprous sulfide (Cu2â^xS) microspheres by a simple template-free route. Inorganic Chemistry Communication, 2003, 6, 1406-1408.	3.9	22
115	Enhanced performance of inverted perovskite solar cells using solution-processed carboxylic potassium salt as cathode buffer layer. Organic Electronics, 2017, 45, 97-103.	2.6	20
116	Establishing Multifunctional Interface Layer of Perovskite Ligand Modified Lead Sulfide Quantum Dots for Improving the Performance and Stability of Perovskite Solar Cells. Small, 2020, 16, e2002628.	10.0	20
117	Sensitively detecting antigen of SARS-CoV-2 by NIR-II fluorescent nanoparticles. Nano Research, 2022, 15, 7313-7319.	10.4	17
118	Methyl functionalization on conjugated side chains for polymer solar cells processed from non-chlorinated solvents. Journal of Materials Chemistry C, 2020, 8, 11532-11539.	5.5	14
119	Concentric Sub-micrometer-Sized Cables Composed of Ni Nanowires and Sub-micrometer-Sized Fullerene Tubes. Advanced Functional Materials, 2007, 17, 1124-1130.	14.9	13
120	The Heck Polycondensation for Functional Polymers. Synlett, 2006, 2006, 2879-2893.	1.8	12
121	Cobalt-N4 macrocyclic complexes for heterogeneous electrocatalysis of the CO2 reduction reaction. Chinese Journal of Catalysis, 2022, 43, 104-109.	14.0	12
122	Template-free fabrication of fullerene (C60, C70) nanometer-sized hollow spheres under solvothermal conditions. Carbon, 2008, 46, 1736-1740.	10.3	10
123	Shielding Unit Engineering of NIR-II Molecular Fluorophores for Improved Fluorescence Performance and Renal Excretion Ability. Frontiers in Chemistry, 2021, 9, 739802.	3.6	10
124	Monodisperse, nanoporous ceria microspheres embedded with Pt nanoparticles: general facile synthesis and catalytic application. RSC Advances, 2014, 4, 42965-42970.	3.6	8
125	Defect-Free Polymer Multilayers Prepared via Chemoselective Immobilization. Langmuir, 2007, 23, 4367-4372.	3.5	7
126	Dithieno[3,2-b:2′,3′-d]pyran-containing organic Dâ€″π–A sensitizers for dye-sensitized solar cells. RSC Advances, 2014, 4, 62472-62475.	3.6	7

#	Article	IF	CITATIONS
127	Organic Spherical Nucleic Acids for the Transport of a NIRâ€Iâ€Emitting Dye Across the Blood–Brain Barrier. Angewandte Chemie, 2020, 132, 9789-9797.	2.0	7
128	Combining ZnO and PDINO as a Thick Cathode Interface Layer for Polymer Solar Cells. ACS Applied Materials & Interfaces, 2022, 14, 18736-18743.	8.0	7
129	In Vivo Imaging: Multiplexed NIRâ€II Probes for Lymph Nodeâ€Invaded Cancer Detection and Imagingâ€Guided Surgery (Adv. Mater. 11/2020). Advanced Materials, 2020, 32, 2070086.	21.0	6
130	Naphthodithiophene-Based Semiconducting Materials for Applications in Organic Solar Cells. Organic Photonics and Photovoltaics, 2014, 2, .	1.3	5
131	Diagnostics: High Performance, Multiplexed Lung Cancer Biomarker Detection on a Plasmonic Gold Chip (Adv. Funct. Mater. 44/2016). Advanced Functional Materials, 2016, 26, 7993-7993.	14.9	5
132	Circulating Tumor Cells: Magnetic "Squashing―of Circulating Tumor Cells on Plasmonic Substrates for Ultrasensitive NIR Fluorescence Detection (Small Methods 2/2019). Small Methods, 2019, 3, 1970004.	8.6	5
133	Tracing the Origin of Visible Light Enhanced Oxygen Evolution Reaction. Advanced Materials Interfaces, 2019, 6, 1801543.	3.7	5
134	Length-dependent self-assembly of oligothiophene derivatives in thin films. Journal of Materials Research, 2011, 26, 296-305.	2.6	4
135	The electron and energy transfer between oligothiophenes and thieno[3,4- b ]thiophene units. Proceedings of SPIE, 2008, , .	0.8	1
136	Large-scale synthesis of single crystal silver nanowires by a sodium diphenylamine sulfonate reduction process. Journal of Nanoscience and Nanotechnology, 2006, 6, 231-4.	0.9	1